Tracking of Synchronization and Desynchronization during the process of Signal Stabilization in a 3×3 Memory Type Nonlinear Systems

KARTIK CHANDRA PATRA[1,a,*], ASUTOSH PATNAIK[2]
Department of Electrical Engineering
C. V. Raman Global University, Bhubaneswar,
Odisha 752054,
INDIA
*Corresponding Author
[a]ORCID ID: 0000-0002-4693-4883

Abstract: - The paper proposes the first harmonic linearization concept leading to a novel graphical technique developed to predict limit cycles (LC) in 3×3 systems with memory-type nonlinearities. This approach leverages computer graphics for ease of visualization and analysis, making the method more accessible and lucid. Under the exhibition of LC, it has been attempted to quench such oscillations by adopting the signal stabilization method with deterministic/random signals. In the process of signal stabilization, tracking of synchronization (alignment of oscillations) and desynchronization (loss of alignment) with deterministic and random signals has been explored. The propositions of the work have been illustrated through an example with backlash type nonlinearities that are commonly present in physical systems on several occasions and in particular in the power system and control system. The proposed graphical method has been validated by digital simulation by means of MATLAB code and with the usage of SIMULINK ToolBox of MATLAB. The developed graphical method in the prediction of LC in 3x3 systems with backlash-type nonlinearities is a novel and significant innovation, making the complex analysis more accessible and interpretable. The work extends to practical applications by proposing ways to stabilize limit cycles using both deterministic and random signals, and tracking synchronization / desynchronization.

Key-Words: - Limit cycles, signal stabilization, describing function, incremental input describing function, synchronization, memory type nonlinearities

Received: April 21, 2024. Revised: November 12, 2024. Accepted: December 15, 2024. Published: March 21, 2025.

1 Introduction

The significance of prediction of Limit cycles (LC) in Multivariable Nonlinear system are widely felt for six or seven decades [1 - 38]. Quenching of such limit cycling oscillation using the method of signal stabilization has gained attention in the beginning of 1960s, [39, 40] and further discussed in [26, 41, 42, 43, 44, 45]. The signal stabilization by high frequency signals either deterministic or random for multivariable systems having memory type nonlinearities is a years old problem. In [46], it has been narrated the process of signal stabilization with determination of stability boundary, synchronization and desynchronization with high frequency signal for 2×2 memory type nonlinear systems. Backlash (a common memory-type nonlinearity) often degrades speed and position control in various applications, including robotics, automation, and load frequency control by Governors in multi area power systems due to exhibition of LC. This has been vividly

discussed for multivariable systems [31, 35, 43, 46, 47, 48, 49, 50, 51, 52, 53].

In the recent literature multidisciplinary applications have been discussed where LC has been addressed. In [55], three possible scenarios such as, stable LC, chaotic behavior arising in the system's flow and thermal dynamics of the system have been discussed. In [56], a cell model has been formulated for the limit cycles. In [57], the nonlinear system's dynamic behavior, switching between a stable equilibrium and a LC, has been demonstrated. In [58], LC has been addressed in an auto catalytic system using Hop bifurcation. In [59] the LC has been predicted and observed in Bio-Oscillators with positive and negative feedback. In [60] an empirical dynamic modelling has been developed in natural systems to present/predict a stable limit cycle.

However, a little literature addresses the analysis of Limit cycling oscillations in 3×3 nonlinear multivariable systems in the past two decades, only [1, 34, 36, 37, 38]. It was felt an important concern

among the researchers to quench the LC in the case of 3×3 nonlinear systems having memory type nonlinearities. In the possible existence of a limit cycle, quenching of oscillations is done by high frequency dither signals. Signal stabilizations using deterministic signals with tracking of Synchronization and Desynchronization has been thoroughly investigated in 2×2 memory type nonlinear systems [46]. An attempt has been made in the present work in tracking the amplitude of stabilizing signal for complete extinction of the limit cycling oscillations during the process of Synchronization and Desynchronization in 3×3 nonlinear systems having Backlash type nonlinearity (memory type). The method uses the describing function (Harmonic Balance) and presents the results from digital simulations. Where, both deterministic and random signals are used as stabilizing signals.

The proposed work is presented in the following sequence, section 2 considers a graphical technique for the investigation of LC in 3×3 systems with memory type nonlinearity following the procedure as depicted in [1]. Section 3 describes the method of digital simulation for the validation of the graphical method of proposition. Section 4 deals with the Signal Stabilization with the special attention for tracking (i) the amplitude of deterministic high frequency sinusoidal signal is varied at a fixed frequency and (ii) the mean value of random (Gaussian) signal is varied at a fixed value of variance. This concept has been demonstrated through a digital simulation of a system with backlash nonlinearity, utilizing the MATLAB/Simulink toolbox.

2 Investigation of LC in 3×3 system through a memory type Nonlinearity

2.1 Graphical Method
Considering the complexity and much involved mathematical analysis a graphical technique [1] is developed for investigation of LC in 3×3 nonlinear systems. Consider a system having three inter connected systems as given in Figure 1. In the system N_1, N_2 & N_3 are 3 nonlinear elements with Backlash characteristics as shown in Figure 2 (a), (b), (c) respectively. $G_1(s)$, $G_2(s)$ and $G_3(s)$ are transfer functions of three linear elements.

The Laplace operator s is replaced by jω in frequency response analysis because this analysis focuses on steady-state outputs resulting from sinusoidal inputs.
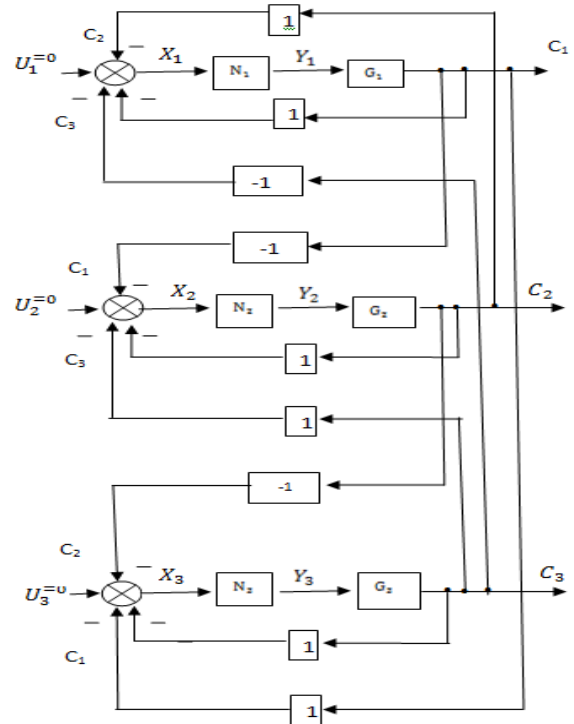

Figure. 1: A class of 3×3 multivariable nonlinear systems

The graphical method based on a normalized phasor diagram [46] has been developed for investigation of LC in a system that is illustrated through an Example. With the intention of reducing complexity of the method the system is presumed to show LC primarily at a single frequency. In Example with memory type nonlinearity (Backlash) contributes additional phase angle to the loop angle of G_1 (jω), G_2 (jω) and G_3 (jω) of the subsystems S_1, S_2 and S_3. By substituting the nonlinear elements with their own Describing Functions (DFs) on basis of harmonic linearization, the exhibition of LC, is possible if the following three conditions are satisfied [1]. For memory type nonlinearities:

(i) The Phase of the Loop should be
$$\theta = 180^o = \angle G_1 + \angle G_2 + \angle G_3 + \angle N_1 + \angle N_2 + \angle N_3$$
where phase angle of G results from jω and phase angle of N results from phase shift of respective DFs.

(ii) The Gain condition: $\frac{C_1}{R_1} \times \frac{C_2}{R_2} \times \frac{C_3}{R_3} = 1$: where

$$\frac{C_1}{R_1} = \frac{G_1(j\omega)N_1(X_{m1}, \omega)}{1 + G_1(j\omega)N_1(X_{m1}, \omega)}$$

$$\frac{C_2}{R_2} = \frac{G_2(j\omega)N_2(X_{m2}, \omega)}{1 + G_2(j\omega)N_2(X_{m2}, \omega)}$$

$$\frac{C_3}{R_3} = \frac{G_3(j\omega)N_3(X_{m3}, \omega)}{1 + G_3(j\omega)N_3(X_{m3}, \omega)}$$
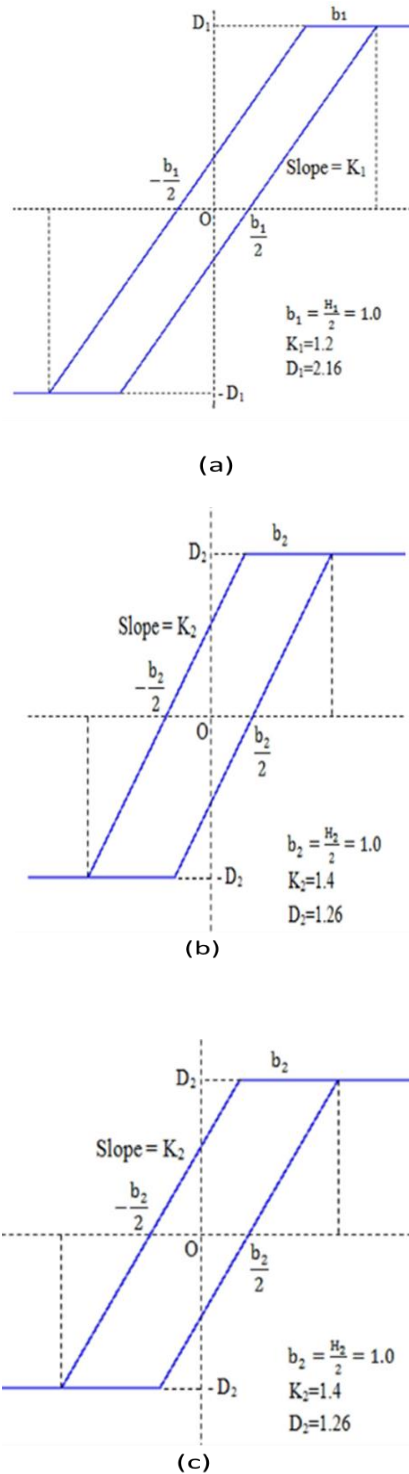
(a)

(b)

(c)

Figure 2: Input and output characteristics of nonlinear elements, N_1, N_2 and N_3

(iii)   The Amplitude Ratio condition:
$\frac{X_1}{X_2} = \frac{V_1}{V_2}; \frac{X_2}{X_3} = \frac{V_2}{V_3}; \frac{X_3}{X_1} = \frac{V_3}{V_1}$ where

$X_1 = X_{m1}; X_2 = X_{m2}; X_3 = X_{m3}$
and
V_1: Eigen Vector corresponds to Eigen Value λ_1 of A (system matrix)

V_2: Eigen Vector corresponds to Eigen Value λ_2 of A (system matrix)

V_3: Eigen Vector corresponds to Eigen Value λ_3 of A (system matrix)

2.2 An Example for Illustration of the Graphical Method in the prediction of LC

Consider the system of Figure. 1 with $G_1(s) = \frac{2}{s(s+1)^2}$; $G_2(s)=\frac{1}{s(s+4)}$; $G_3(s)=\frac{1}{s(s+2)}$ and the three nonlinear elements with backlash characteristics using $b_1=b_2=b_3=1.0$, and slopes $K_1=1.2$, $K_2=K_3=1.4$ are stated in Figure.2.(a), 2(b) and 2(c).

DFs as mentioned above Backlash Nonlinearities are expressed as:

$N(X_m,\omega)= \left| \frac{Y}{Xm} < \phi \right|$ ……………… (1), [1]

or

$N(X_m,\omega)=\frac{\frac{KXm}{\pi}\sqrt{(\frac{\pi}{2}+\beta+\frac{1}{2}sin2\beta)^2+\cos^4\beta}}{Xm}$ *

$\angle$- $\tan^{-1}\left(\frac{\cos^2\beta}{\frac{\pi}{2}+\beta_1+\frac{1}{2}sin2\beta}\right)$

or

$N(Xm,\omega) = \left\{\frac{K}{\pi}\sqrt{(\frac{\pi}{2}+\beta+\frac{1}{2}sin2\beta)^2+\cos^4\beta}\right\}$

$\angle - \tan^{-1}\left(\frac{\cos^2\beta}{\frac{\pi}{2}+\beta+\frac{1}{2}sin2\beta}\right)$ for $Xm > \frac{b}{2}$ ⋯ ⋯ (2)

$= 0$ $for\ X_m < \frac{b}{2}$

and $N_1(Xm,\omega)=\frac{K_1}{\pi}\sqrt{(\frac{\pi}{2}+\beta_1+\frac{1}{2}sin2\beta_1)^2+\cos^4\beta_1}$
… (3) and

$N_2(Xm_2,\omega)=\frac{K_2}{\pi}\sqrt{(\frac{\pi}{2}+\beta_2+\frac{1}{2}sin2\beta_2)^2+\cos^4\beta_2}$
… (4) and

$N_3(Xm_3,\omega) = \frac{K_3}{\pi}\sqrt{(\frac{\pi}{2}+\beta_3+\frac{1}{2}sin2\beta_3)^2+\cos^4\beta_3}$
… (5)

The derivative of the DF comes out to be:

$N_1'(X_{m1},\omega) = \frac{K_1}{\pi}\times\frac{1}{\sqrt{(\frac{\pi}{2}+\beta_1+^1/_2\sin2\beta_1)^2+\cos^4\beta_1}}\times(2\times(\frac{\pi}{2}+$

$\beta_1+\frac{1}{2}\sin2\beta_1)+(1+\cos2\beta_1)+2\times(\cos2\beta_1+1)\times$
$(-2sin^2\beta_1))$ ……   (6)

$f_1(X_{m1}) = \frac{K_1}{\pi}\sqrt{(\frac{\pi}{2}+\beta_1+^1/_2\sin2\beta_1)^2+\cos^4\beta_1}-N_1(X_{m1})$
                    (7)

$$f_1'(X_{m1}) = \frac{K_1}{\pi} \times \frac{1}{\sqrt{(\frac{\pi}{2}+\beta_1+^1/_2 \sin 2\beta_1)^2 + \cos^4\beta_1}} \times (2 \times (\frac{\pi}{2} + \beta_1 +$$
$$\frac{1}{2}\sin 2\beta_1) + (1 + \cos 2\beta_1) + 2 \times (\cos 2\beta_1 + 1) \times$$
$$(-2\sin^2\beta_1)) N_1'(X_{m1}) \qquad (8)$$

Again, $\quad N_2(X_{m2}, \omega) = \frac{K_2}{\pi}\sqrt{(\frac{\pi}{2} + \beta_2 + ^1/_2 \sin 2\beta_2)^2 + \cos^4\beta_2}$
$$(9)$$

The derivative of the DF comes out to be:

$$N_2'(X_{m2}, \omega) = \frac{K_2}{\pi} \times \frac{1}{\sqrt{(\frac{\pi}{2}+\beta_2+^1/_2 \sin 2\beta_2)^2 + \cos^4\beta_2}} \times (2 \times (\frac{\pi}{2} +$$
$$\beta_2 + \frac{1}{2}\sin 2\beta_2) + (1 + \cos 2\beta_2) + 2 \times (\cos 2\beta_2 + 1) \times$$
$$(-2\sin^2\beta_2)) \qquad (10)$$

$$f_2(X_{m2}) = \frac{K_2}{\pi}\sqrt{(\frac{\pi}{2} + \beta_2 + ^1/_2 \sin 2\beta_2)^2 + \cos^4\beta_2} - N_2(X_{m2})$$
$$(11)$$

$$f_2'(X_{m2}) = \frac{K_1}{\pi} \times \frac{1}{\sqrt{(\frac{\pi}{2}+\beta_2+^1/_2 \sin 2\beta_2)^2+\cos^4\beta_2}} \times (2 (\frac{\pi}{2} + \beta_2 +$$
$$\frac{1}{2}\sin 2\beta_2) + (1 + \cos 2\beta_2) + 2(\cos 2\beta_2 + 1) \times$$
$$(-2\sin^2\beta_2)) - N_1'(X_{m1}) \qquad (12)$$

Because the relationships between N_1 and X_1, N_2 and X_2, and N_3 and X_3 are implicit (or transcendental, or based on memory), the third of the three alternative procedures, [1], has to be adopted for obtaining the solution. Eqn. (7); Eqn. (9) and Eqn. (11) contain absolute values of N_1; N_2 and N_3 respectively. At a fixed value of ω, N_1, N_2 and N_3 are constants. The $\frac{X_2}{X_1}$ and $\frac{X_3}{X_1}$ ratios are determined from and Newton Raphson (N R) method which are compared with that of $\frac{X_2}{X_1}$ and $\frac{X_3}{X_1}$ ratio obtained from graphical plot and at $\omega = 0.57$ (c f Table. 1 a) they match and confirm the existence of a limit cycle.

The Newton-Raphson (NR) method, when applied to solve Equations (3), (4), and (5), disregards phase angles during iteration. However, these angles are subsequently incorporated into the loop angles, as shown in Equations (13), (14), and (15). However, for every iteration step, the phase angle condition (cf Eqn. (i): phase $\theta = 180^o = \angle G_1 + \angle G_2 + \angle G_3 + \angle N_1 + \angle N_2 + \angle N_3$: Three combinations are used to create the normalized phase diagrams, for example:
Combination 1: Subsystems S_1, S_2 & S_3; C_1 positive, C_2 negative, C_3 positive, shown in Figure 3(a).
Combination 2: Subsystems S_2, S_3 & S_1: C_1 positive, C_2 positive, C_3 negative, shown in Figure 3(b).
Combination 3: Subsystems S_1, S_3 & S_2: C_1 negative, C_2 positive, C_3 positive, shown in Figure 3(c).
Figure 3(a) represents normalised phase diagram with C_1, C_2 and C_3 for combination 1, C_1 positive, C_2 negative, C_3 positive.
Table 1: shows the r (radius), θL_1 , θL_2 , θL_3 , , and the crossing point of the state lines and the circle for

combinations 1, 2 and 3 (see Example). It may be noted that Table 1(a): contain the values of $\frac{Xm2}{Xm1} = \frac{Xm3}{Xm1}$ for different values of ω using NR method as well as from the graphical plots of Normalised Phase Diagrams. When $\frac{Xm2}{Xm1}$ both are matched equal, confirms the LC with the corresponding frequency $\theta L_1 = \theta N_1(Xm_1, \omega) + \theta G_1$, $\theta L_2 = \theta N_2(Xm_2, \omega) + \theta G_2$, $\theta L_3 = \theta N_3(Xm_3, \omega) + \theta G_3$, $r_1 = \frac{1}{2\sin\theta L_1}$ and Centre $C(\frac{1}{2}) - \frac{1}{2\tan\theta L_1}$ for combination 1:

$$\theta_{L_1} = [-tan^{-1}\left(\frac{\cos^2\beta_1}{\frac{\pi}{2}+\beta_1+\frac{1}{2}\sin^2\beta_1}\right) - \frac{\pi}{2} - 2tan^{-1}\omega],$$
$$\beta_1 = \sin^{-1}(1 - \frac{b_1}{X_{m1}}); \qquad (13)$$

$$; \quad \theta_{L_2} = [-tan^{-1}\left(\frac{\cos^2\beta_2}{\frac{\pi}{2}+\beta_2+\frac{1}{2}\sin^2\beta_2}\right) - \frac{\pi}{2} - tan^{-1}\frac{\omega}{4}],$$
$$\beta_2 = \sin^{-1}(1 - \frac{b_2}{X_{m2}}) \qquad (14)$$

$$\theta_{L_3} = [-tan^{-1}\left(\frac{\cos^2\beta_3}{\frac{\pi}{2}+\beta_3+\frac{1}{2}\sin^2\beta_3}\right) - \frac{\pi}{2} - tan^{-1}\frac{\omega}{2}],$$
$$\beta_3 = \sin^{-1}(1 - \frac{b_3}{X_{m3}}) \qquad (15)$$

For subsystem (s_1): $\theta_{L_1} = \theta_{N_1(X_{m1},\omega)} + \theta_{G_1(j\omega)}$

Similarly, for subsystem (s_2): $\theta_{L_2} = \theta_{N_2(X_{m2},\omega)} + \theta_{G_2(j\omega)}$

for subsystem (s_3): $\theta_{L_3} = \theta_{N_3(X_{m3},\omega)} + \theta_{G_3(j\omega)}$

In the light of the normalized phase diagrams, [46], for 3×3 systems, the limit cycling condition are drawn with 3 combinations shown in Figure 3(a), (b), (c):
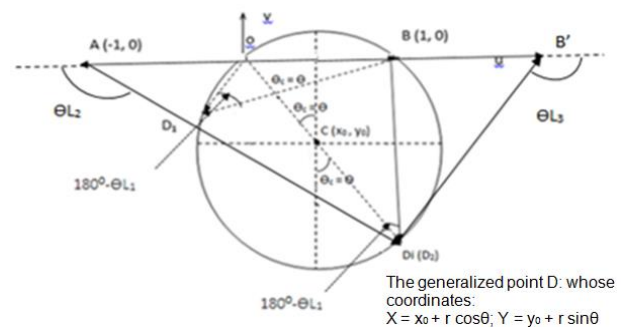

Figure 3 (a): Normalized phase diagram (combination 1: C_1 positive, C_2 negative, C_3 positive).
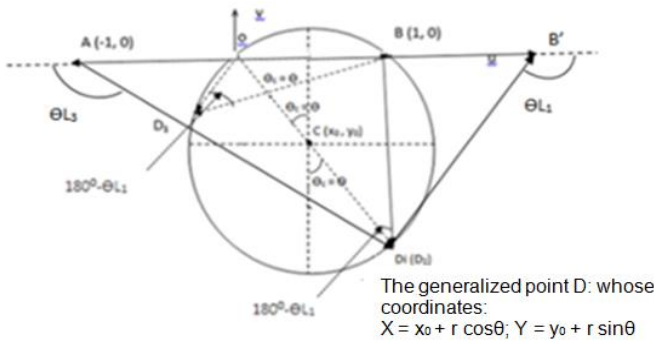
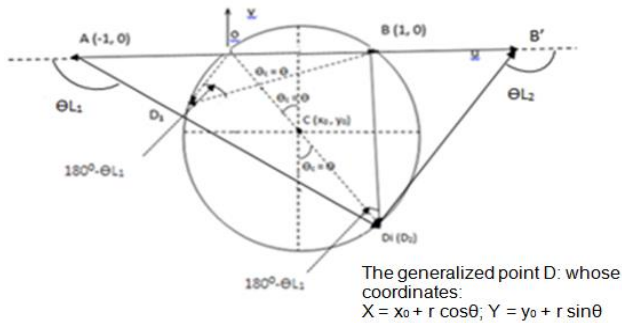Figure 3 (b): Normalized phase diagram for combination 2 (C_1 positive, C_2 positive, C_3 negative).

Figure 3 (c): Normalized phase diagram for combination 2 (C_1 negative, C_2 positive, C_3 positive).

Table 1 (a): Shows ω, N_1 , N_2 , N_3, X_{m1}, X_{m2}, X_{m3}, θL_1, θL_2, θL_3 , r (radius), and centre of the circle for combination 1 for the example (Backlash).

$$\frac{X_2}{X_1} = \frac{AD\prime}{BD\prime} \text{ from graphical plot } \dots\dots\dots\dots \text{ (16)}$$

$$\frac{X_{m2}}{X_{m1}} = \frac{X_2}{X_1} \text{ from N.R. method i.e. from Table 6 (a) (17)}$$

$$\frac{X_3}{X_1} = \frac{B\prime D\prime}{BD\prime} \text{ from graphical plot } \dots\dots\dots\dots \text{ (18)}$$

$$\frac{X_{m3}}{X_{m1}} = \frac{X_3}{X_1} \text{ from N.R. method i.e. from Table1(a) …(19)}$$

Table 1b: Shows r (radius), and centre of the circle for combination 1 for example (Backlash), X_{m2}/X_{m1} = AD/BD′ (from plot), X_{m2}/X_{m1} (from Table), X_3 / X_1 = B′D′/ BD′

3 Digital Simulation

3.1. Numerical problems

The Example is revisited: A 3×3 system presented in Figure 1 has 3 nonlinear elements as given in Figure 2 correspondingly and 3 linear transfer functions are.

$$G_1(s) = \frac{2}{s(s+1)^2} \; ; G_2(s) = \frac{2}{s(s+4)} \text{ and } G_3(s) = \frac{1}{s(s+2)}$$

Partial Fraction Expansion of $G_1(s)$, $G_2(s)$ and $G_3(s)$:

$$G_1(s) = \frac{A}{s} + \frac{B}{s+1} + \frac{C}{(s+1)^2} = \frac{A(s+1)^2 + Bs(s+1) + Cs}{s(s+1)^2}$$

$$Or \frac{s^2(A+B) + s(2A+B+C) + A}{s(s+1)^2} = \frac{2}{s(s+1)^2}$$

Or A+B=0, A=2,: 2A+B+C=0, B=-A =-2,: C=-2A-B=-4+2=-2

Hence $G_1(s) = \dfrac{2}{s} - \dfrac{2}{s+1} - \dfrac{2}{(s+1)^2} : \dfrac{2}{s}, \dfrac{-2}{s+1}, \dfrac{-2}{s+1}\left(\dfrac{1}{s+1}\right)$

$$G_2(s) = \frac{1}{s(s+4)} = \frac{A}{s} + \frac{B}{(s+4)} = \frac{A(s+4) + Bs}{s(s+4)}$$

$$= \frac{4A + s(A+B)}{s(s+4)}$$

$$Or\ 4A = 1 : A = \frac{1}{4}, A+B = 0 : B = -A = -\frac{1}{4}$$

Hence $G_2(s) = \dfrac{0.25}{s} - \dfrac{0.25}{s+4}$

$$G_3(s) = \frac{1}{s(s+2)} = \frac{A}{s} + \frac{B}{s+2} = \frac{A(s+2) + Bs}{s(s+2)}$$

$$= \frac{2A + (B+A)s}{s(s+2)}$$

$$Or\ 2A = 1 : A = \frac{1}{2}, A+B = 0 : B = -A = -\frac{1}{2}.$$

Hence $G_3(s) = \dfrac{0.5}{s} - \dfrac{0.5}{s+2}$

For a small sampling duration T, TG(z) approximates G(s). Figure 4 & 5 show canonical and digital equivalents of Figure 1 for the Example.
Z-transfer functions from Laplace functions:

$$G_1(s): \frac{2}{s} \Rightarrow \frac{2z}{z-1} ; \frac{-2}{s+1} \Rightarrow \frac{-2z}{z-e^{-T}} ; \frac{-2}{(s+1)^2} \Rightarrow \frac{-2Tz\,e^{-T}}{(z-e^{-T})^2}$$

$$G_2(s): \frac{0.25}{s} \Rightarrow \frac{0.25z}{(z-1)} ; \frac{-0.25}{s+4} \Rightarrow \frac{-0.25z}{z-e^{-4T}} ;$$

$$G_3(s): 0.5/s \Rightarrow 0.5z/(z-1); -0.5/(s+2) \Rightarrow -0.5z/(z-e^{-2T})$$

Table 1a: Values of different quantities for the Example (Backlash)

| ω	N₁	N₂	N₃	Xm1	Xm2	Xm3	θL1	θL2	θL3	Radius r	$\frac{X_{m2}}{X_{m1}}$ From Table	$\frac{X_{m3}}{X_{m1}}$ From Table
0.525	1.302	1.262	1.262	3.85	2.85	2.85	-154.45	-110.83	-117.81	-1.182		
0.550	1.114	1.251	1.251	3.57	2.55	2.55	-157.99	-112.51	-120.05	-1.324		
0.570	**1.290**	**1.230**	**1.230**	**3.30**	**2.30**	**2.30**	**-160.62**	**-114.38**	**-122.18**	**-1.510**	**0.93**	**0.93**
0.575	1.286	1.225	1.225	3.27	2.25	2.25	-161.15	-114.80	-122.66	-1.550		
0.600	0.252	1.7160	1.7160	2.97	1.95	1.95	-164.44	-117.60	-128.36	-1.865	0.65	0.65
0.625	0.284	1.790	1.790	2.63	1.67	1.67	-168.16	-120.1	-129.38		0.63	0.63
0.650	0.319	1.862	1.862	2.34	1.47	1.47	-172.04	-123.9	-132.72		0.62	0.62
0.675	0.311	2.576	2.576	2.34	1.43	1.43	-174.03	-124.9	-133.99		0.61	0.61
0.6955	0.305	3.244	3.244	2.34	1.47	1.4	-175.63	-125.19	-134.51		0.628	0.628
0.6961	0.305	3.263	3.263	2.34	1.43	1.4	-175.67	-125.2	-134.52		0.610	0.610
0.7000	0.3055	3.3844	3.3844	2.340	1.43	1.43	-175.975	-125.26	-134.62		0.628	
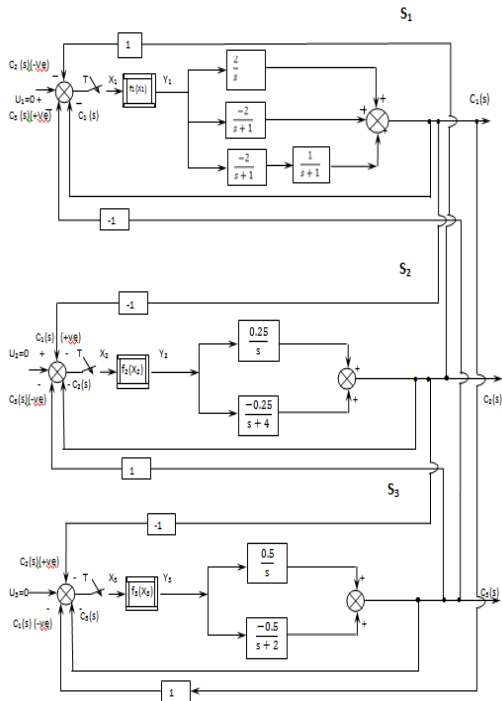
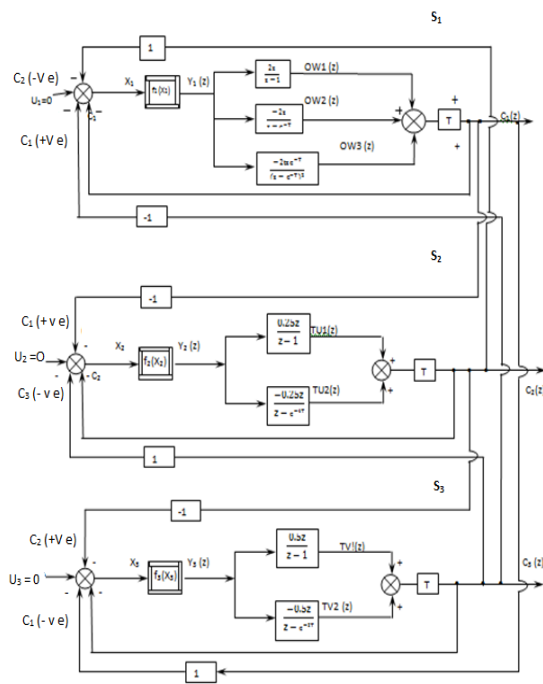Figure 4: Canonical form of the Example in Figure 1

Figure 5: The Digital representation of Figure 1 for the Example

Table 1b Normalized Phase diagrams for different values of ω and its corresponding r for the Example (Backlash) using graphical methods.

ω	Radius r	Centre $(0.5, \dfrac{-1}{2\tan\theta_{L_1}})$	$\dfrac{X_{m2}}{X_{m1}}$ from plot	$\dfrac{X_{m2}}{X_{m1}}$ from Table 6a	$\dfrac{X_{m3}}{X_{m1}}$ from plot	$\dfrac{X_{m3}}{X_{m1}}$ From Table 6a	Phasor Diagram
0.525	-1.182	0.5, -1.073		0.740			
0.550	-1.324	0.5, -1.237		0.714			
0.570	**-1.506**	**0.5, -1.42**	**1.07**	**1.07**	**1.13**	**1.13**	
0.600	-1.865	0.5, -1.797		0.657			
0.625	2.4387	0.5, -2.387		0.636			

Kartik Chandra Patra, Asutosh Patnaik

From the Figure 4 following algorithm has been derived:

(1) $\dfrac{OW1(z)}{Y_1(z)} = \dfrac{2z}{z-1} \Rightarrow 2Y_1(z) = \dfrac{z-1}{z}OW1(z)$
$= OW1(z) - z^{-1}OW1(z)$

Finding z^{-1}: OW1 (n T) = $2Y_1$ (n T) + OW1$(\overline{n-1}T)$

(2) $\dfrac{OW2(z)}{Y_1(z)} = \dfrac{-2z}{z-e^{-T}} \Rightarrow -2Y_1(z)$
$= \dfrac{z-e^{-T}}{z}OW2(z)$
$= OW2(z) - z^{-1}e^{-T}OW2(z)$

Finding z^{-1} transform: OW2 (nT) = $-2Y_1$ (nT) $+e^{-T}$ OW2$(\overline{n-1}T)$

(3) $\dfrac{OW3(z)}{Y_1(z)} = \dfrac{-2Tze^{-T}}{(z-e^{-T})^2} \Rightarrow -2Tze^{-T}Y_1(z) =$
$\dfrac{(z-e^{-T})^2}{z}OW3(z) = z^*OW3(z) - 2e^{-T}OW3(z) +$
$e^{-2T}z^{-1}OW3(z)$

Or $-2Te^{-T}z^{-1}Y_1(z) = OW3$ (z) $-2e^{-T}z^{-1}OW3$ (z) $+ e^{-2T}z^{-2}$ OW3 (z)

Finding z^{-1} transform: OW3 (nT) = $-2Te^{-T}Y_1(\overline{n-1}T) + 2e^{-T}$ OW3$(\overline{n-1}T)$ $- e^{-2T}OW3(\overline{n-2}T)$

(4) $\dfrac{TU1(z)}{Y_2(z)} = \dfrac{0.25z}{(z-1)} \Rightarrow 0.25 Y_2(z)$
$= \dfrac{z-1}{z}TU1(z) - z^{-1}TU1(z)$

Finding z^{-1} transform: TU1 (nT) = $0.25Y_2$ (nT) $+TU1(\overline{n-1}T)$

(5) $\dfrac{TU2(z)}{Y_2(z)} = \dfrac{-0.25z}{(z-e^{-4T})} \Rightarrow -0.25 Y_2(z) = \dfrac{z-e^{-4T}}{z}TU2(z) =$
$TU2(z) - z^{-1}e^{-4T}TU2(z)$

Finding z^{-1} transform: TU2 (nT) = $-0.25Y_2$ (nT) $+ e^{-4T}TU2(\overline{n-1}T)$

(6) $\dfrac{TV1(z)}{Y_3(z)} = \dfrac{0.5z}{(z-1)} \Rightarrow 0.5 Y_3(z) = \dfrac{z-1}{z}TV1(z) =$
$TV1(z) - z^{-1}TV1(z)$

Finding z^{-1} transform: TV1 (nT) $=0.5Y_3$ (n T) $+TV1(\overline{n-1}T)$

(7) $\dfrac{TV2(z)}{Y_3(z)} = \dfrac{-0.5z}{(z-e^{-2T})} \Rightarrow -0.5 Y_3(z) = \dfrac{z-e^{-2T}}{z}TV2(z) =$
$TV2(z) - z^{-1}*AK2*TV2(z)$

Finding z^{-1} transform: TV2 (nT) = $-0.5Y_3$ (nT) + AK2* TV2$(\overline{n-1}T)$

Let us take $(\overline{n-1}T)$ is the 0th instant; nT is the 1st instant, so we can write:

OW1$(\overline{n-1}T)$ = OW1N$\phi \Rightarrow$OW1N; OW1 (nT) = OW1N1; OW2$(\overline{n-1}T)$ = OW2N$\phi \Rightarrow$OW2N; OW2 (nT) = OW2N1

Now C_1 (nT) = OWN1 = T* [OW1N1 + OW2N1 + OW3N1] = T* [OW1 (nT) +OW2 (nT) + Ow3 (nT)]
$=T*[2Y_1$ (nT) + OW1N-$2Y_1$ (nT)+ AK*OW2N– 2*T* AK1 * 0Y1N + 2*AK1*OW3N - AK2*OW3 NN]
$=$OWN1$=C_1$

OW3$(\overline{n-2}T)$ = OW3N (-1)$\Rightarrow$OW3NN; OW3 $(\overline{n-1}T)$ = OW3N$\phi \Rightarrow$ OW3N ; OW3 (nT)=OW3N1

Similarly,
TU1$(\overline{n-1}T)$ = TU1N$\phi \Rightarrow$ TU1N; TU1 (nT) = TU1N1, TU2$(\overline{n-1}T)$ = TU2N$\phi=$ TU2N; TU2 (nT) = TU2N1

Now C_2 (nT) =TUN1= T*[TU1 (nT) + TU2 (nT)] = T* [0.25 Y_2 (nT) + TU1N – 0.25Y_2 (nT) + AK3*TU2N] = TUN1 = C_2

Similarly,
TV1$(\overline{n-1}T)$ = TV1N$\phi \Rightarrow$ TV1N; TV1 (nT) = TV1N1
TV2$(\overline{n-1}T)$ = TV2N$\phi \Rightarrow$ TV2N; TV2 (nT) = TV2N1
Now C_3 (n T) = TVN1 = T*[TV1 (nT) + TV2 (nT)]
$=$ T*[0.5Y3 (nT) + AK2* TV2N+ TV1N-0.5Y3 (nT)] = TVN1 = C_3

Next Run:
$\qquad R_1$=ORN1=$C_3 - C_2$ =TVN1 – TUN1
$\qquad R_2$ = TRN1 = $C_1 - C_3$ = OWN1 – TVN1
$\qquad R_3$ = THRN1= $C_2 - C_1$ = TUN1 – OWN1
X_1 = OXN1 = ORN1 – OWN1,
X_2 = TXN1 = TRN1 – TUN1,
X_3 = THXN1 = THRN1 – TVN1

3.2. Utilizing the SIMULINK Tool Box of MATLAB

Using the SIMULINK Toolbox, X_1, X_2, X_3, C_1, C_2, and C_3 were calculated for the backlash example (Fig. 6). A comparison was then performed between these SIMULINK results and those obtained from graphical and digital simulations.

A MATLAB program implementing the algorithm produced the results shown in Figure 7. Figures 7(a) and 7(b) present the digital simulation and SIMULINK Toolbox results, respectively, for the Example. Table 2a provides the corresponding numerical values.
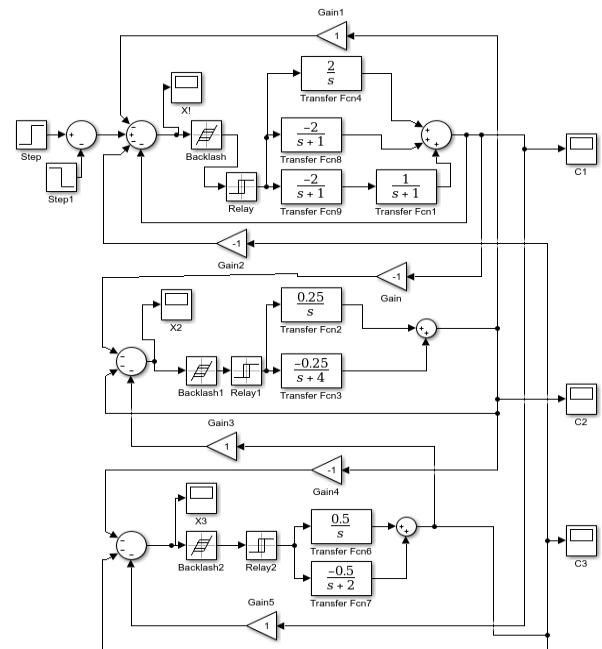

Figure 6 shows the SIMULINK model for predicting LC in the backlash example.
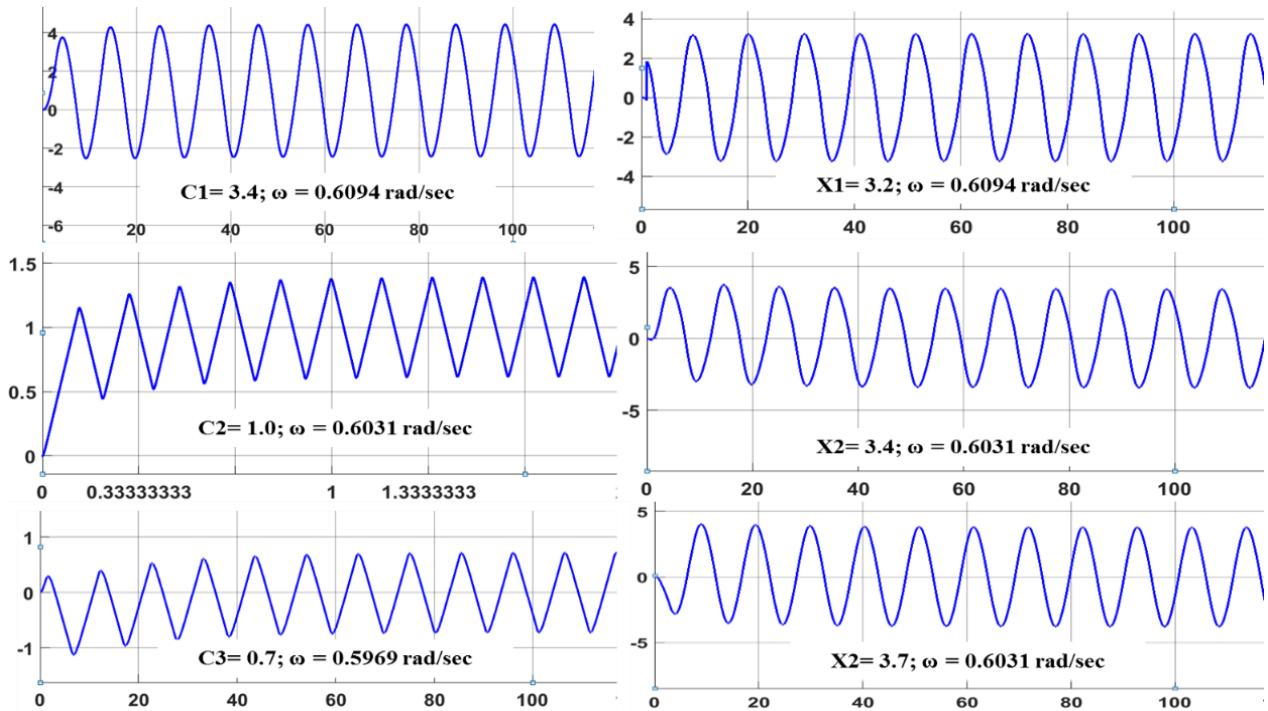
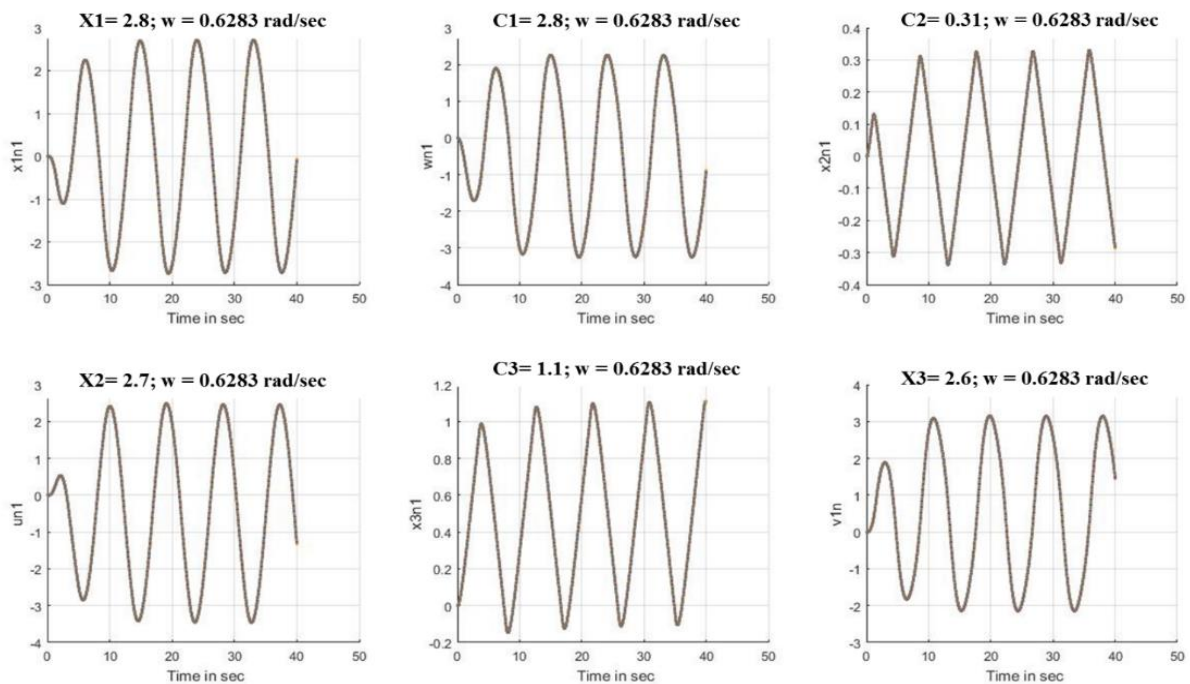Figure 7 (a): SIMULINK results and images for C_1, X_1, C_2, X_2, C_3, and X_3 of the Example (Backlash).

Figure 7 (b): Simulation results and images for C_1, X_1, C_2, X_2, C_3, and X_3 of the Example (Backlash)

Table.2.: Results for the backlash example using different methods

Sl. No	Techniques	C_1	C_2	C_3	X_1	X_2	X_3	ω
1	Graphical	2.94	1.00	1.00	3.00	3.20	3.37	0.57
2	Digital Simulation	2.80	0.31	1.10	2.80	2.70	2.60	0.62
3	Use of SIMULINK TOOL BOX OF MATLAB	3.40	1.00	0.70	3.20	3.40	3.70	0.60

4 Signal stabilization in 3×3 systems with Backlash nonlinearity

4.1 Usage of Deterministic signal

After establishing the presence of a limit cycle (LC) in the autonomous system of Figure 1 (backlash example), LC quenching was explored by inserting a high-frequency signal (greater than ten times the LC frequency) [39] at one or all three input points (U_1, U_2, U_3). Gradually increasing the amplitude (B_1) of one sinusoidal input ($B1 \sin \omega_f t$), while holding the amplitudes of other forcing signals ($B_2 \sin \omega_f t$ and $B_3 \sin \omega_f t$) fixed or at zero, led to complex oscillations [46]. The system's variables then comprised signals at the forcing frequency (ω_f), the self-oscillation frequency (ω_s), and combinations thereof ($k_1\omega_f \pm k_2\omega_s$, where k_1 and k_2 are integers) [46].

With all three inputs (U_1, U_2, U_3) at $B \sin \omega_f t$ (Figure 8, backlash example), gradually increasing B caused the limit cycle (LC) oscillation frequency (ω_s) changing until synchronization with the forcing frequency (ω_f) occurred. This quenched the LC, resulting in forced oscillations at ω_f. The synchronization (LC quenching) occurred at B1. The numerical values are shown in Table 3 and the images at the Synchronization point are shown in Fig. 8. If the amplitude B is then decreased, a value (B_2) will be reached where the LC reappears (desynchronization occurs, and the system oscillates at ω_s). It has been seen that generally the value B_2 (Desynchronization) is smaller than B_1 (Synchronization). During signal stabilization (forced oscillations), the system's low-pass characteristics cause the outputs C_1, C_2, and C_3 to be negligibly small. The inputs to nonlinear elements

N_1, N_2, and N_3 can be closely approximated by B sign $\omega_f t$ plus a negligible signal. Step-by-step reduction of B results in the re-appearance of self-oscillations [46, 48] as the forced oscillations lose stability. This instability can be explored using the Incremental Input Describing Function (IDF) [9, 12]. The threshold value of B for the reappearance of self-oscillations is found by replacing the nonlinear elements N_1, N_2, and N_3 with corresponding IDFs. $N_{1i} = K_1$, $N_{2i} = K_2$, and $N_{3i} = K_3$, where K_1, K_2, and K_3 are the slopes of the nonlinear elements [26, 46, 48].
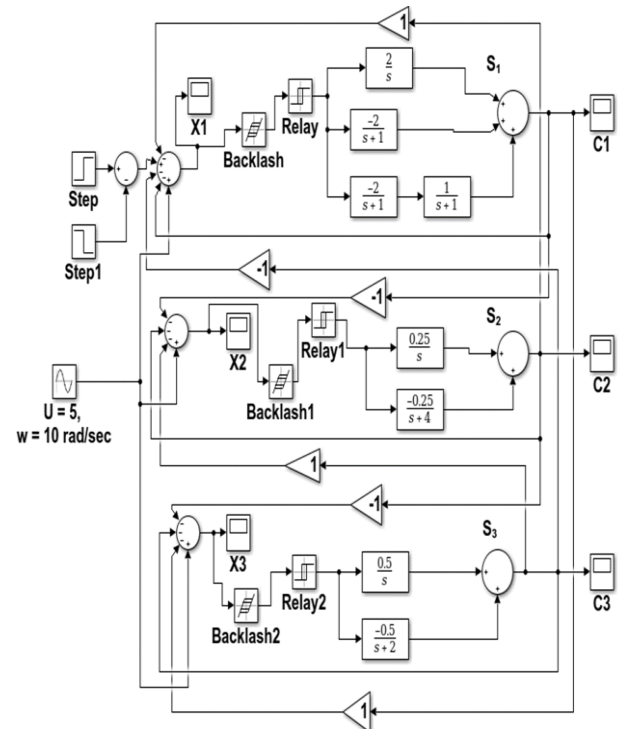

Figure 8: The equivalent system for signal stabilization of the backlash example using a deterministic input B sin $\omega_f t$ (rad/sec) as shown in Figure 1.

The Simulation results and images for signal stabilization with deterministic signals in the Example shown in Figure 9.

The steady state results are indicated as C_{1ss}, C_{2ss}, C_{3ss} and X_{1ss}, X_{2ss}, X_{3ss} with their frequencies, $\omega = \omega_f$.

Kartik Chandra Patra, Asutosh Patnaik

Table 3: Results of Simulink for the Example (Backlash) showing Synchronization (Deterministic Signals).

U	C1	C2	C3	X1	X2	X3	ω
0	3.6	0.985	1.4	3.6	3.8	4.1	0.54
0.5	3.2	0.9	1.3	3.5	3.1	4.05	0.58
1.0	3.2	0.9	1.2	3.5	3.0	4.5	0.58
1.5	2.54	1.0	1.02	4.2	4.2	4.2	0.65
2.0	2.45	1.0	0.9	3.2	3.5	4.0	0.64
2.5	0.001	0.001	0.001	2.5	2.5	3.9	10.0
3.0	**0**	**0**	**0**	**2.9**	**3.0**	**3.0**	**10.0**
3.5	0	0	0	3.4	3.4	3.4	10.1

Table 4: Results of Simulink for the Example (Backlash) showing Tracking of Stabilizing signals for complete extinction of LC (Gaussian Signals) at Mean = 500 and Variance = 0.06

Mean	Variance	C1	C2	C3	X1	X2	X3	ω
0	0	3.68	0.995	1.42	3.6	3.8	4.1	0.559
1	0	3.6	0.98	1.4	3.6	3.8	4.1	0.552
2	0	3.58	0.70	1.4	3.1	2.7	4.0	0.534
2.5	0.02	3.48	0.34	1.43	3.3	2.7	3.9	0.552
3.0	0.02	3.4	0.36	1.4	3.3	3.8	4.1	0.559
5.0	0.02	3.35	0.34	1.37	3.4	3.5	3.9	0.559
10.0	0.02	3.48	0.24	1.35	2.9	3.4	3.9	0.527
20.0	0.02	2.97	0.2	1.3	2.9	2.4	3.3	0.508
30.0	0.02	2.97	0.34	1.58	3.0	3.4	3.7	0.584
50.0	0.02	3.26	0	1.58	3.1	3.4	3.7	0.565
100	0.02	0.11	0	0.75	3.2	3.6	3.8	0.565
150	0.02	3.00	0	0.8	2.9	1.9	3.1	0.640
200	0.02	2.8	0	0.8	3.3	1.4	3.6	0.584
250	0.02	3.2	0	1.6	2.0	3.3	3.3	0.615
300	0.02	3.3	0	1.6	1.9	3.0	3.5	0.609
300	0.025	3.4	0	1.5	1.5	3.0	3.1	0.584
300	0.03	3.0	0	0.75	1.5	2.75	3.3	0.584
300	0.035	3.2	0	0.75	1.5	2.5	3.1	0.653
300	0.04	2.1	0	0.65	1.4	2.5	3.4	0.603
300	0.05	2.9	0	1.0	1.5	2.0	3.3	0.578
500	**0.06**	**0**	**0**	**0**	**0**	**0**	**0**	**0**
510	0.06	0	0	0	0	0	0	0

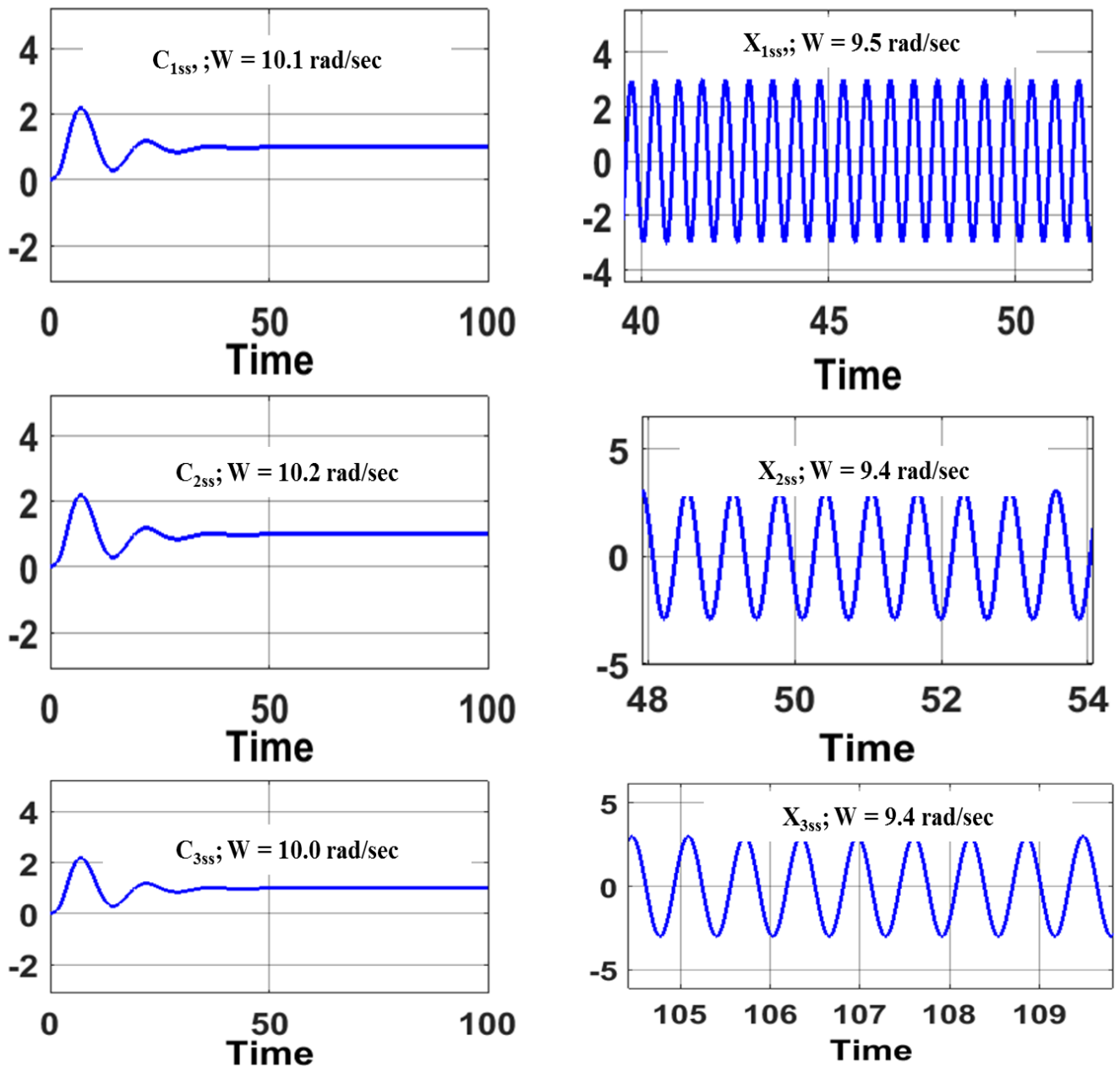Figure 9: Signal stabilization with a deterministic forcing signal ($U = 3.0 \sin \omega t$, $\omega_f = 10.0$ rad/sec) induced forced oscillations in the backlash example

4.2 Using Random/Gaussian signal

Signal stabilization using Gaussian signals in single input single output (SISO) nonlinear system has been discussed in [40, 44, 45]. While robust design and analysis considering uncertainty/randomness are important, signal stabilization with Gaussian signals for multivariable systems with memory-type nonlinearity (even 2×2) was lacking until [50]. This work attempts to quench the LC in 3×3 nonlinear systems using a random signal.

The backlash example is revisited. Under autonomous conditions, the system exhibits a limit cycle (LC). To stabilize the system/quench these self-sustained oscillations, a Gaussian/random signal with varying mean (m) and fixed variance (φ) was injected at inputs U_1, U_2, and U_3 (Figure 10). At the specific values of m and φ where the system synchronized with the high-frequency forcing input, LCs were no longer present. Table 4 shows the steady-state values (mean/variance) at which LC quenching occurred, and Figure 11 presents simulation/Simulink images of the system at this point.
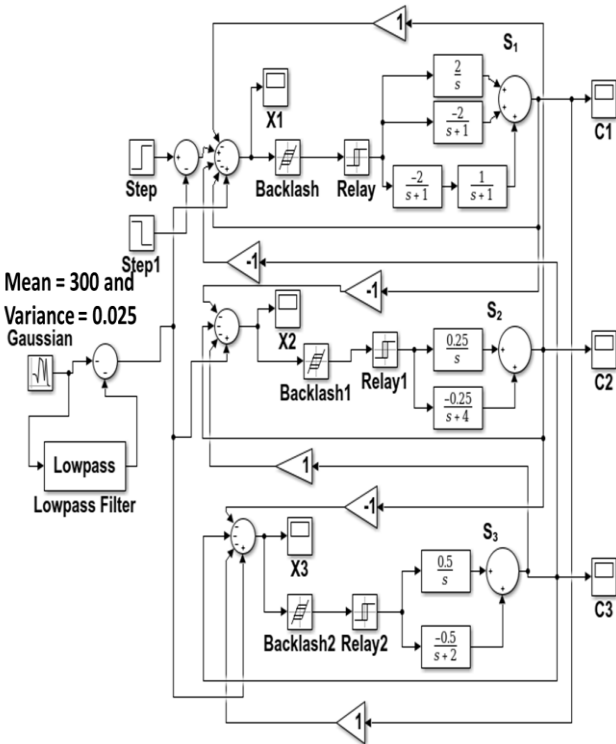
Figure 10: A system with backlash, driven by a Gaussian signal with a normal distribution (mean 300, variance 0.025), seeking output stabilization.
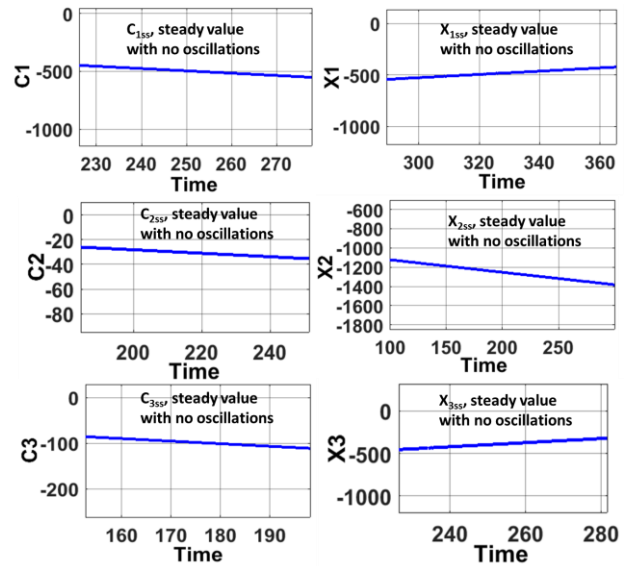
Figure 11: A system with backlash subjected to forced oscillations from a Gaussian signal (mean 500, variance 0.06) with output stabilization.

5 Conclusion

Limit cycles (LCs) indicate instability, and these nonlinear self-sustained oscillations degrade speed and position control performance in robot technology, automation, and load frequency control in power systems. Limited research exists on quenching LCs in 2×2 systems with memory-type nonlinearities. Whereas the present paper explores the complete extinction of LC using the methods of signal stabilization in 3×3 systems with memory type nonlinearities. The proposed graphical method facilitates a better insight into the problem because of its simplicity in applications. The novelty and significant innovation of the present effort claims in: (i) complete extinction of LC by signal stabilization with (a) deterministic signals, (b) random signals – robust applications which addresses uncertainties, (ii) (a) In the process of signal stabilization, tracking of the amplitude of deterministic signals with high frequency ω_f at least ten times the limit cycling frequency ω_s ($\omega_f \approx 10\omega_s$) has been applied to determine the point of synchronization and desynchronization, (b) similar tracking has also been done with random signals.

There is a bright scope of extending the work of tracking to determine synchronization and desynchronization including the determination of stability boundary for n × n multivariable nonlinear systems. Most importantly, the limiting value of stabilizing signal (deterministic) in the reverse process (desynchronization) can easily be accessed

Kartik Chandra Patra, Asutosh Patnaik

using the IDFs which are real values even for memory type nonlinearities.

References:

[1]. PATRA, K. C, PATNAIK, A, Investigation of the Existence of Limit Cycles in Multi Variable Nonlinear Systems with Special Attention to 3x3 Systems. Int. Journal of Applied Mathematics, Computational Science and System Engineering. Vol. 5, 2023, pp. 93-114.

[2]. NORDIN, M. and Gutman, P. O Controlling mechanical systems with backlash- a survey, Automatica, vol. 38, (10), 2002, pp.1633-1649.

[3]. WANG, C, et al, Analysis and suppression of limit cycle oscillation for Transmission System with backlash Nonlinearity, IEEE Transactions on Industrial Electronics, vol. 62, (12), 2017, pp. 9261-9270.

[4]. GELB, A, Limit cycles in symmetric multiple nonlinear systems. IEEE Trans. Autumn. Control: AC-8, 1963, pp. 177-178.

[5]. JUD, H.G Limit cycle determination of parallel linear and non- linear elements. IEEE Trans. Autumn. Control: AC-9, 1964, pp. 183-184.

[6]. GRAN, R., and RIMER, M Stability analysis of systems with multiple nonlinearities. IEEE Trans. Autumn. Control: 10, 1965, pp. 94-97.

[7]. DAVISON, E.J., and CONSTANTINESCU, D Describing function technique for multiple nonlinearity in a single feedback system IEEE Trans Autumn. Control: AC-16: 1971, pp. 50-60

[8]. VISWANDHAM, N., and DEEKSHATULU, B.L Stability analysis of nonlinear multivariable systems. Int. J. Control, 5, 1966, pp. 369-375.

[9]. GELB, A. and VADER-VELDE, W.E Multiple-input describing functions and nonlinear system design, McGraw- Hill, New York, 1968

[10]. NIKIFORUK, P.N., and WINTONYK, B.L.M Frequency response analysis of two-dimensional nonlinear symmetrical and non-symmetrical control systems. Int. J. Control, 7, 1968, pp.49- 62.

[11]. RAJU, G.S., and JOSSELSON, R Stability of reactor control systems in coupled core reactors, IEEE Trans. Nuclear Science, NS-18, 1971, pp. 388-394.

[12]. ATHERTON, D.P Non-linear control engineering - Describing function analysis and design. Van Noslrand Reinhold, London, 1975

[13]. ATHERTON, D.P., and DORRAH, H.T A survey on nonlinear oscillations, Int. J. Control, 31. (6), 1980, pp. 1041-1105.

[14]. GRAY, J. O. And NAKHALA, N.B Prediction of limit cycles in multivariable nonlinear systems. Proc. IEE, Part-D, 128, 1981 pp. 233-241.

[15]. MEES, A. I Describing function: Ten years on. IMA J. Appl. Math., 34, 1984 pp. 221-233.

[16]. SEBASTIAN, L the self-oscillation determination to a category of nonlinear closed loop systems, IEEE Trans. Autumn. Control, AC-30, (7), 1985 pp. 700-704.

[17]. COOK, P. A Nonlinear dynamical system, Prentice-Hall, Englewood ClilTs, NJ, 1986

[18]. CHANG, H.C., PAN, C.T., HUANG, C.L., and WEI, C.C A general approach for constructing the limit cycle loci of multiple nonlinearity systems, IEEE Trans. Autumn. Control, AC-32, (9), 1987, pp. 845-848.

[19]. PARLOS, A.G., HENRY, A.F., SCHWEPPE, F.C., GOULD, L.A., and LANNING, D.D Nonlinear multivariable control of nuclear power plants based on the unknown but bounded disturbance model, IEEE Trans. Autumn. Control, AC-33, (2), 1988 pp. 130-134.

[20]. PILLAI, V.K., and NELSON, H.D A new algorithm for limit cycle analysis of nonlinear systems, Trans. ASME, J. Dyn. Syst. Meas. Control, 110, 1988, pp. 272-277.

[21]. GENESIO, R., and TESI, A On limit cycles of feedback polynomial systems, IEEE Trans. Circuits Syst., 35, (12), 1988, pp. 1523-1528.

[22]. FENDRICH, O.R Describing functions and limit cycles, IEEE Trans. Autom. Control, AC - 31, (4), 1992, pp. 486487.

[23]. PATRA, K.C., and SINGH, Y.P Structural formulation and prediction of limit cycle for multivariable nonlinear system. IETE, Tech. Rev. India, 40, (5 & 6), 1994, pp. 253-260.

[24]. ZHUANG, M., and ARTHERTON, D.P PID controller design lor TITO system, TEE Proc. Control Theory Appl. 141, (2), 1994, pp. 111-120.

[25]. LOH, A.P., and VASANU, V.V Necessary conditions for limit cycles in multi loop relay systems, IEE Proc., Control Theory Appl., 141, 31, 1994, pp. 163-168.

[26]. PATRA, K.C., et al Prediction of limit cycles in nonlinear multivariable systems, Arch. Control Sci. Poland, 6(XLII),7N.1-2 1997, pages 89 to 102.

[27].NNAJI, A. C., ABONYI, D.O. AND IYIDOBI, J.C, Prediction of Limit Cycles in Systems with Friction Using Describing Function Analysis Technique. Journal of Innovative Engineering and Technology Volume: 04, Nov:02/September 2021, pp. 9-19

[28].TESI, A, et al Harmonic balance analysis of periodic doubling bifurcations with implications for control of nonlinear dynamics, Automatic, 32 (9), 1996, 1255, 1271.

[29].HORI, Y. et al Slow resonance ratio control for vibration suppression and disturbance rejection in torsional system, IEEE Trans. Ind. Electron., vol. 46, (1), 1999, pp.162-168.

[30].LIN, C.H., HAN, K.W Prediction of Limit cycle in Nonlinear two input two output control system, 'IEE Proc.-Control Theory Appl. Vol.146, No.3 may. 1999.

[31].CHIDAMBARAM, I.A, and VELUSAMI, S Decentralized biased controllers for load-frequency control of inter connected power systems considering governor dead band non-linearity, INDICON, Annual IEEE, 2005, pp.521-525.

[32].EFTEKHARI, M and KATEBI, S. D Evolutionary Search for Limit Cycle and Controller Design in Multivariable non-linear systems, Asian Journal of Control, , Vol. 8, No. 4, 2006, pp. 345 – 358.

[33].KATEBI, M, et al Limit Cycle Prediction Based on Evolutionary Multi objective Formulation, Hindawi Publishing Corporation, Mathematical Problems in engineering Volume, Article ID 816707, 2009, 17pgs.

[34].GARRIDO, J, et al Centralized PID control by Decoupling of a Boiler-Turbine Unit, Proceedings of the European Control Conference, Budapest, Hungary, Aug. 2009, 23-26.

[35].TSAY, T.S Load Frequency control of interconnected power system with governor backlash nonlinearities, Electrical Power and Energy, vol. 33, 2011, pp.1542-1549.

[36].TSAY, T.S Limit Cycle prediction of nonlinear multivariable feedback control systems with large transportation lags, Hindawi Publishing corporation journal of control science and Engineering, Vol., article id 169848, 2011.

[37].TSAY, T.S Stability Analysis of Non-linear Multivariable Feedback Control systems, WSEAS Transactions on systems, Volume 11, Issue 4, 2012, pp. 140 – 151.

[38].SUJATHA, V., PANDA, R. C Relay Feedback Based Time domain modelling of Linear 3-by-3 MIMO System, American Journal of System Science, Scientific & Academic Publishing, 1(2) 2012, pp. 17-22.

[39].OLDENBURGER, R., T. NAKADA T Signal stabilisation of self - oscillating system IRE Trans. Automat Control. USA, 6, 1961, pp: 319-325.

[40].OLDENBURGER, R., SRIDHAR, R., "Signal Stabilization of a Control System with Random Input". Journals & Magazines: Transactions of the American Institute of Electrical Engineers. Part II: Applications and Industry; Vol.80, Issue 5, 1961, pp 260-268

[41].SHI, Z, and ZUO, Z back stepping control for gear transmission servo systems with backlash nonlinearity IEEE Trans. Autumn. Sci. Eng., vol. 12, (2), 2015, pp. 752-757.

[42].KERAN, S, XIAOLONG, W and RONGWEI, G. Stabilization of Nonlinear Systems with External Disturbances Using the DE-Based Control Method Symmetry (MDPI), 15, 987,2023

[43].ZEINEB, R., CHEKIB, G. and NACEUR, B.B Non-Fragile H_ Stabilizing Nonlinear Systems Described by Multivariable Hammerstein Models Nonlinear Dynamics of Complex Systems, Hindawi (Special Issue) Volume 2021,19 Feb. 2021,

[44].SRIDHAR, R., OLDENBURGER, R., "Stability of a Nonlinear feedback system in the presence of Gaussian Noise", ASME Trans., 1962, Journal of Basic Engineering, 84, pp. 61-70.

[45].GIBSON, J. E., SRIDHAR, R., "The Response of Nonlinear closed-loop Systems to Random Inputs", ASME Trans., 1964, Journal of Basic Engineering, pp. 132-138.

[46].PATRA, K. C, and DAKUA, B. K, Investigation of limit cycles and signal stabilisation of two dimensional systems with memory type nonlinear elements, Archives of Control Sciences, vol. 28, (2), 2018, pp. 285-330.

[47].RAJAGOPALAN, P. K and MISHRA, J: Dual input describing function of double-valued Nonlinearities, In Proceedings of Institution of Electrical Engineers, IET, 116(10), (1969, October),1764-1768

[48].RAJ GOPALAN, P. K and SINGH, Y. P. Analysis of harmonics and almost periodic oscillations in forced self-oscillating systems, Proc 4th IFAC Congress, Warsaw. 41, (1969), 80-122

[49].LIM, L. H and LOH, A.P. Forced and sub-harmonic oscillations in relay feedback systems, Journal of the Institution of Engineers Singapore, 45(5),(2005),pp88-100

[50]. PATRA, K. C, KAR, N Signal Stabilization of Limit cycling two Dimensional Memory Type Nonlinear Systems by Gaussian Random Signal, International Journal of Emerging Trends & Technology in Computer Science, Vol.9 Issue 1, 2020, pp.10-17

[51]. HABIB, G, and KERSCHEN, G. Suppression of limit cycle oscillations using the nonlinear tuned vibration absorber. Mathematical Physical and Engineering Sciences, 08 April 2015 https://dol.org

[52]. WANG, C, et al Vibration suppression with shaft torque limitation using explicit MPC-PI switching control in elastic drive systems, IEEE Trans. Ind. Electron, vol. 62,(11), 2015, pp. 6855-6867.

[53]. YANG, M, et al Suppression of mechanical resonance using torque disturbance observer for two inertia system with backlash Proc. IEEE 9th Int. Conf. Power Electron., ECCE Asia, 2015, pp. 1860 - 1866.

[54]. ELISABETH, T. M & SENG, C. C. Designing Limit-Cycle Suppressor Using Dithering and Dual-Input Describing Function Methods. Mathematics, Vol.8(MDPI) No.6,2020

[55]. LOPEZ, D.S, VEGA, A.P, Fuzzy Control of a Toroidal Thermosyphon for Known Heat Flux Heating Conditions, Proceeding of the 8th World Congress on Momentum, Heat and Mass Transfer (MHMT'23), Lisbon Portugal-March 26-28, 2023. DOI:10.11159/enfht23.133

[56]. CORRADO. C, et. al, Quantifying the impact of shape uncertainty on predict arrhythmias, Computers in Biology and Medicine, Elsevier Ltd., 153, 2023, 106528.

[57]. CHEN, W., et. al, Oscillation characteristics and trajectory stability region analysis method of hierarchical control microgrids, Energy Reports, 9, 2023, pp 315-324.

[58]. Kumar, U., et.al. The effect of sub diffusion on the stability of autocatalytic systems, Chemical Engineering Science, Elsevier Ltd., 265, 2023, 118230.

[59]. Marrone, J.I., et.al. A nested bistable module within a negative feedback loop ensures different types of oscillations in signalling systems, Scientific reports| Nature portfolio, 2023, 13:529.

[60]. MUNCH, S, B., et.al. Recent developments in empirical dynamic modelling, Methods in Ecology and Evolution, 2022, 14, pp 732-745.

Contribution of Individual Authors to the Creation of a Scientific Article (Ghostwriting Policy)

The authors equally contributed in the present research, at all stages from the formulation of the problem to the final findings and solution.

Conflict of Interest

The authors have no conflicts of interest to declare that are relevant to the content of this article.